 doi:10.20944/preprints202211.0100.v1

On the dynamic interaction of social processes and COVID-19 infection dynamics

F. Nyabadza[1]*, J. Mushanyu[1,2], R. Mbogo[3], G. Muchatibaya[2]
[1]Department of Mathematics and Applied Mathematics
University of Johannesburg, South Africa
[2] Department of Mathematics and Computational Sciences
University of Zimbabwe, Zimbabwe,
[3]Institute of Mathematical Sciences,
Strathmore University, Kenya

Abstract

Human behaviour was tipped as the mainstay in the control of further SARS-CoV-2 (COVID-19) spread especially after the lifting of restrictions by many countries. Countries in which restrictions were lifted soon after the first wave, had subsequent waves of the COVID-19 infections and it remains to be seen whether there will be more waves. In this paper, we formulate a deterministic model for COVID-19 incorporating dynamic non-pharmaceutical interventions, dubbed social dynamics. The model steady states are determined and their stability analysed. Numerical simulations are carried out to determine the pack of various parameters that influence the social dynamics. In South Africa, the first wave was the only wave in which the only interventions rested solely on human behavior. The model is thus fitted to COVID-19 data on the first wave in South Africa. The results presented in this paper have implications on the trajectory of the pandemic in the presence of changing social processes.

Keywords: COVID-19, mathematical modelling, stability, dynamic social processes, simulations.

1 Introduction

COVID-19 has infected nearly 500 million people and 6.2 million people have died as a results of the pandemic as of 8 April 2022 [32]. The COVID-19 outbreak is likely to be the largest pandemic of the 21st century, in terms of human lives lost [24]. While vaccines have resulted in some notable disease control, with declines in infected cases globally, there is currently very few specific medical interventions, only in developing countries, see for instance [20]. For developing countries such

*Corresponding author: fnyabadza@uj.ac.za

 doi:10.20944/preprints202211.0100.v1

as South Africa, classes of drugs that are mainly used include antiviral agents, inflammation inhibitors, low-molecular-weight heparins, plasma, and hyperimmune immunoglobulins [26]. In the absence of effective infection prevention and control measures, human behaviour that reduces or prevents exposure to the virus is key [21].

The role played by mathematical models in the infection dynamics of COVID-19 cannot be underestimated. Many of the public health policies to contain the global pandemic of COVID-19 have been driven by mathematical models, that have been to a large extent regional or country specific, see for instance [15, 33] for Wuhan, China, [11] for Italy, [8, 13] for Spain, [12, 18] for the United Kingdom, [27] for Scotland and [6, 28] for the United States of America, to mention a few. The challenges of modelling the global pandemic have also been looked at by a number of authors, see for instance[4, 23, 31]. One of the biggest problems in modelling infectious diseases, is the inclusion of human behaviour in the models. The role of human behavior in modulating the spread and prevalence of COVID-19 was presented in [1] using the imitation dynamic approach of evolutionary game theory. Human behaviour plays a very crucial role in the way infectious diseases spread and it is the understanding of how the behaviour influences disease spread that is key to devising and improving control measures. [2, 10].

The emergence of second waves of COVID-19 has been linked to the interplay between the infection dynamics and psycho-social processes within communities [9, 22]. The first waves of COVID-19, often referred to as the “herald waves”, see [25], have been followed by a second and third waves of the viral infection months after the initial episodes. The subsequent waves have been more parlous than the first one and this has been observed in other pandemics such as the influenza pandemics of 1918, 1957, 1968, and 2009 [9].

In this paper, we explore the role of two important aspects in the dynamics of the pandemic that have evolved over time, i.e information and non-pharmaceutical interventions (NPIs). NPIs that have involved aspects such as social distancing, wearing of masks, restrictions generally known as "lockdowns", have been touted as the best measures to reduce the spread of COVID-19 to date. The possible resurgence of other respiratory endemic infections due to the NPIs has been predicted in [3]. The aim is to investigate how time dependent information translates into the growth or decline of NPIs that in turn impact the transmission of COVID-19. Many mathematical models have considered NPIs modelled by constant parameters, see for instance [19]. This work presented in this paper follows the research in [7], but unlike in [7], we focus on the long term dynamics of the infection, the role of information and its potential impact in influencing NPIs.

This paper is arranged as follows: In section 1, the introduction to the paper is presented followed by the model formulation in section 2. The model analysis is presented in section 3. Numerical simulations are presented in section 4 and section 5 concludes the paper.

Preprints (www.preprints.org) | NOT PEER-REVIEWED | Posted: 7 November 2022 doi:10.20944/preprints202211.0100.v1

2 Mathematical model

We consider a classical human $SEIR$ model, coupled with behavioural state variables of: susceptible individuals $S(t)$, exposed individuals who are not yet infectious $E(t)$, and infectious individuals who are either detected $I_d(t)$ or undetected $I_u(t)$, recovered individuals who are either recorded $R_d(t)$ or unrecorded $R_u(t)$. The total human population is given by

$$N(t) = S(t) + E(t) + I_d(t) + I_u(t) + R_d(t) + R_u(t).$$

The social processes at any time t are modelled by two state variables, $\epsilon(t)$ and $\rho(t)$, where $\epsilon(t)$ models the information on the disease, mainly driven by the number of detected cases that are then reported in the media and $\rho(t)$ models the NPIs (personal hygiene, travel bans, mass gatherings bans, social distancing, curfews, and lockdowns) that are used to reduce transmission, and are also driven by the changes in the information on COVID-19. We assume that $0 < \epsilon(t), \rho(t) \leq 1$.

The human population increases through births at a rate μN, with recruits assumed susceptible and μ being the birth/death rate. The susceptibles are infected through interaction with the infected in the compartments I_d and I_u at a rate λ defined by

$$\lambda = \beta(1 - \rho(t))\frac{(I_d(t) + \eta I_u(t))}{N(t)},$$

where β is the effective contact rate and η is the relative infectivity rate of those in the compartment I_u when compared to those in compartment I_d. Once infected, susceptible individuals move to the exposed class where they progress to become infectious after 5 to 6 days [16] at a rate κ. A proportion q will be undetected infectives while the remaining proportion becomes detected. The detected/undetected infectives recover at rates σ_d/σ_u, and die due to COVID-19 at rates δ_d/δ_u.

The information growth rate is driven by the number of detected cases at a rate α_2 and the information decreases at a rate ν_2 with ϵ_0 being the constant baseline information that the population has. The NPIs grow at a rate α_1 and decrease at a rate ν_1 and the constant baseline value of NPIs practiced by the population are modeled by ρ_0. The model flow diagram is presented in Figure 1 below.

Preprints (www.preprints.org) | NOT PEER-REVIEWED | Posted: 7 November 2022 doi:10.20944/preprints202211.0100.v1

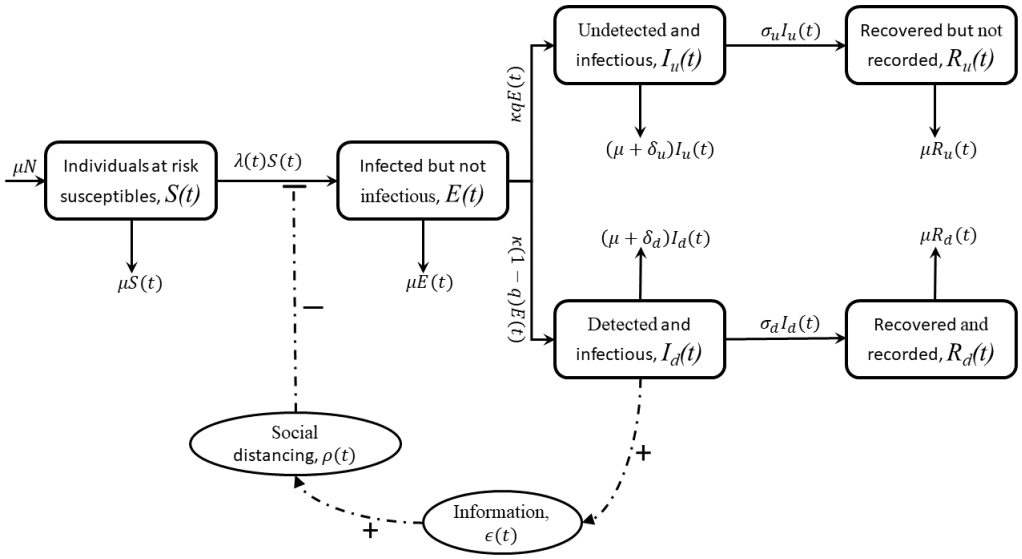

Figure 1: Model diagram

The model formulation summary above together with the model flow diagram (Figure 1) leads to the following system of equations:

$$\begin{cases} \dot{S} &= \mu N - \lambda S - \mu S, & \dot{R}_u &= \sigma_u I_u - \mu R_u, \\ \dot{E} &= \lambda S - (\mu + \kappa)E, & \dot{R}_d &= \sigma_d I_d - \mu R_d, \\ \dot{I}_d &= (1-q)\kappa E - (\mu + \sigma_d + \delta_d)I_d, & \dot{\rho} &= \rho_0 + \alpha_1 \epsilon - \nu_1 \rho, \\ \dot{I}_u &= q\kappa E - (\mu + \sigma_u + \delta_u)I_u, & \dot{\epsilon} &= \epsilon_0 + \alpha_2 I_d - \nu_2 \epsilon. \end{cases} \tag{1}$$

Given that the human population and the social process have different dimension, we re-scale the human population by setting

$$s = \frac{S}{N},\ e = \frac{E}{N},\ i_u = \frac{I_u}{N},\ i_d = \frac{I_d}{N},\ r_u = \frac{R_u}{N} \text{ and } r_d = \frac{R_d}{N}$$

and obtain the following system of differential equations:

$$\left.\begin{aligned} \dot{s} &= \mu - \beta(1-\rho)(i_d + \eta i_u)s - \mu s, \\ \dot{e} &= \beta(1-\rho)(i_d + \eta i_u)s - (\mu + \kappa)e, \\ \dot{i}_d &= (1-q)\kappa e - (\mu + \sigma_d + \delta_d)i_d, \\ \dot{i}_u &= q\kappa e - (\mu + \sigma_u + \delta_u)i_u, \\ \dot{r}_d &= \sigma_d i_d - \mu r_d, \\ \dot{r}_u &= \sigma_u i_u - \mu r_u, \end{aligned}\right\} \cdots \text{Human dynamics} \tag{2}$$

$$\left.\begin{aligned} \dot{\rho} &= \rho_0 + \alpha_1 \epsilon - \nu_1 \rho, \\ \dot{\epsilon} &= \epsilon_0 + \alpha_2 i_d - \nu_2 \epsilon, \end{aligned}\right\} \cdots\cdots\cdots\cdots\cdots \text{Social dynamics} \tag{3}$$

with the initial conditions $s(0) > 0$, $e(0) \geq 0$, $i_d(0) \geq 0$, $i_u(0) \geq 0$, $r_d(0) \geq 0$, $r_u(0) \geq 0$, $\rho(0) > 0$ and $\epsilon(0) > 0$.

Preprints (www.preprints.org) | NOT PEER-REVIEWED | Posted: 7 November 2022 doi:10.20944/preprints202211.0100.v1

3 Model analysis

3.1 Positivity of the solutions

Lemma 1. *Suppose that* $s(0) > 0$, $e(0) \geq 0$, $i_d(0) \geq 0$, $i_u(0) \geq 0$, $r_d(0) \geq 0$, $r_u(0) \geq 0$, $\rho(0) > 0$ *and* $\epsilon(0) > 0$, *then the solution* $(s(t),\ e(t),\ i_d(t),\ i_u(t),\ r_d(t),\ r_u(t),\ \rho(t),\ \epsilon(t)) \in \mathbb{R}^8$ *of system (2)-(3) is positive for all time* $t \geq 0$.

Proof. Let $(s(t),\ e(t),\ i_d(t),\ i_u(t),\ r_d(t),\ r_u(t),\ \rho(t),\ \epsilon(t))$ be the solution of system (2)-(3). From the first equation of system (2)-(3) we have that

$$\dot{s} = \mu - \beta(1-\rho)(i_d + \eta i_u)s - \mu s, \quad \text{where} \quad \tilde{\lambda} = \beta(1-\rho)(i_d + \eta i_u).$$

Thus,

$$\dot{s} = \mu - (\tilde{\lambda} + \mu)s \quad \Rightarrow \quad \dot{s} \geq -(\tilde{\lambda} + \mu)s. \tag{4}$$

Integrating both sides and applying the initial conditions leads to

$$s(t) \geq s(0)e^{-\left(\int_0^t \tilde{\lambda}(\tau)d\tau + \mu t\right)} \tag{5}$$

at any value of $t \geq 0$. Since $s(0) \geq 0$ then $s(t) \geq 0$.
Also, from the second equation of system (2)-(3) we have that

$$\dot{e} = \beta(1-\rho)(i_d + \eta i_u)s - (\mu + \kappa)e \quad \Rightarrow \quad \dot{e} \geq -(\mu + \kappa)e. \tag{6}$$

Integrating both sides and applying the initial conditions gives

$$e(t) \geq e(0)e^{-(\mu+\kappa)t} \tag{7}$$

at any value of $t \geq 0$. Since $e(0) \geq 0$ then $e(t) \geq 0$.
Similarly, it can be shown that $i_d(t) \geq 0$, $i_u(t) \geq 0$, $r_d(t) \geq 0$, $r_u(t) \geq 0$, $\rho(t) \geq 0$ and $\epsilon(t) \geq 0$.

□

3.2 Feasible region

Consider the biological feasible region given by
$\Omega = \left\{\mathcal{X} \in \mathbb{R}^8_+ : n \leq 1, \rho \leq \frac{\rho_0}{\nu_1} + \frac{\alpha_1}{\nu_1\nu_2}(\epsilon_0 + \alpha_2), \epsilon \leq \frac{1}{\nu_2}(\epsilon_0 + \alpha_2)\right\}$, where
$\mathcal{X} = (s(t), e(t), i_u(t), i_d(t), r_u(t), r_d(t), \rho(t), \epsilon(t)), \quad n = s + e + i_u + i_d + r_u + r_d.$

Lemma 2. *The solution of the system (2)-(3) with the non-negative initial conditions are bounded for all* $t \geq 0$ *in the biological feasible region* Ω.

Proof. We note from system (2) that,

$$\frac{dn}{dt} = \mu(1-n) \quad \Rightarrow \quad n(t) = 1 + (n(0) - 1)e^{-\mu t} \tag{8}$$

Preprints (www.preprints.org) | NOT PEER-REVIEWED | Posted: 7 November 2022 doi:10.20944/preprints202211.0100.v1

upon solving the differential equation and applying the initial condition.
Thus, $n \to 1$ as $t \to \infty$.
Also, from system (3) we have that

$$\dot{\epsilon} = \epsilon_0 + \alpha_2 i_d - \nu_2 \epsilon \leq \epsilon_0 + \alpha_2 - \nu_2 \epsilon \quad \text{since} \quad i_d \leq 1. \tag{9}$$

Upon solving the differential inequality (9) we obtain

$$\epsilon(t) \leq \frac{1}{\nu_2}(\epsilon_0 + \alpha_2) + \left(\epsilon(0) - \frac{1}{\nu_2}(\epsilon_0 + \alpha_2)\right) e^{-\nu_2 t}. \tag{10}$$

Thus, as $t \to \infty$ we have that $\epsilon(t) \leq \frac{1}{\nu_2}(\epsilon_0 + \alpha_2)$.
Lastly, from system (3) we have that

$$\dot{\rho} = \rho_0 + \alpha_1 \epsilon - \nu_1 \rho \leq \rho_0 + \frac{\alpha_1}{\nu_2}(\epsilon_0 + \alpha_2) - \nu_1 \rho \quad \text{since} \quad \epsilon \leq \frac{1}{\nu_2}(\epsilon_0 + \alpha_2). \tag{11}$$

Solving the differential inequality (11) we obtain

$$\rho(t) \leq \frac{\rho_0}{\nu_1} + \frac{\alpha_1}{\nu_1 \nu_2}(\epsilon_0 + \alpha_2) + \left(\rho(0) - \frac{\rho_0}{\nu_1} + \frac{\alpha_1}{\nu_1 \nu_2}(\epsilon_0 + \alpha_2)\right) e^{-\nu_1 t}. \tag{12}$$

Thus, as $t \to \infty$ we have that $\rho(t) \leq \frac{\rho_0}{\nu_1} + \frac{\alpha_1}{\nu_1 \nu_2}(\epsilon_0 + \alpha_2)$. Hence $(s, e, i_u, i_d, r_u, r_d, \rho, \epsilon)$ are all bounded in the region Ω. Therefore Ω is biologically feasible. □

3.3 Disease-free equilibrium and model reproduction number

Model system (2)-(3) has a disease-free equilibrium given by

$$\mathcal{D}^0 = \left(s^0, e^0, i_u^0, i_d^0, r_u^0, r_d^0, \rho^0, \epsilon^0\right) = \left(1, 0, 0, 0, 0, 0, \Phi, \frac{\epsilon_0}{\nu_2}\right).$$

Following the next generation matrix approach in van den Driesche and Watmough [30] we have that

$$F = \begin{pmatrix} 0 & \beta(1-\Phi) & \beta\eta(1-\Phi) & 0 & 0 & 0 & 0 \\ 0 & 0 & 0 & 0 & 0 & 0 & 0 \\ 0 & 0 & 0 & 0 & 0 & 0 & 0 \\ 0 & 0 & 0 & 0 & 0 & 0 & 0 \\ 0 & 0 & 0 & 0 & 0 & 0 & 0 \\ 0 & 0 & 0 & 0 & 0 & 0 & 0 \\ 0 & 0 & 0 & 0 & 0 & 0 & 0 \end{pmatrix}$$

and

$$V = \begin{pmatrix} \kappa + \mu & 0 & 0 & 0 & 0 & 0 & 0 \\ -(1-q)\kappa & h_d & 0 & 0 & 0 & 0 & 0 \\ -q\kappa & 0 & h_u & 0 & 0 & 0 & 0 \\ 0 & -\sigma_d & 0 & \mu & 0 & 0 & 0 \\ 0 & 0 & -\sigma_u & 0 & \mu & 0 & 0 \\ 0 & 0 & 0 & 0 & 0 & \nu_1 & -\alpha_1 \\ 0 & -\alpha_2 & 0 & 0 & 0 & 0 & \nu_2 \end{pmatrix}.$$

Preprints (www.preprints.org) | NOT PEER-REVIEWED | Posted: 7 November 2022 doi:10.20944/preprints202211.0100.v1

Thus, the basic reproduction number denoted by $\mathcal{R}_0$ and defined as the spectral radius of the matrix FV^{-1} is given by

$$\begin{aligned} \mathcal{R}_0 &= \mathcal{R}_d + \mathcal{R}_u \quad \text{with} \\ \mathcal{R}_d &= \frac{\beta\kappa(1-\Phi)(1-q)}{(\mu+\kappa)h_d} \quad \text{and} \quad \mathcal{R}_u = \frac{\beta\kappa(1-\Phi)q\eta}{(\mu+\kappa)h_u}, \end{aligned} \tag{13}$$

where $h_d = \mu+\sigma_d+\delta_d$, $h_u = \mu+\sigma_u+\delta_u$ and $\Phi = \dfrac{\rho_0\nu_2 + \epsilon_0\alpha_1}{\nu_1\nu_2}$. We fix $\Phi < 1$ in order for $\mathcal{R}_0$ to be biologically meaningful. Here, $\mathcal{R}_d$ and $\mathcal{R}_u$ represent the contribution of individuals in classes i_d and i_u respectively.

3.4 Endemic equilibrium

The long term dynamics of the model can be determined by considering the steady states of the model. Solving the first, third, fourth, fifth and sixth equations of system (2) together with equations for system (3) in terms of e^* gives

$$\begin{cases} s^* &= 1 - \dfrac{e^*(\mu+\kappa)}{\mu}, \quad i_u^* = \dfrac{e^*\kappa q}{h_u}, \quad i_d = \dfrac{e^*\kappa(1-q)}{h_d}, \quad r_u^* = \dfrac{e^*\kappa q\sigma_u}{\mu h_u}, \\ r_d^* &= \dfrac{e^*\kappa(1-q)\sigma_d}{\mu h_d}, \quad \epsilon^* = \dfrac{\epsilon_0 h_d + \alpha_2 e^*\kappa(1-q)}{\nu_2 h_d}, \\ \rho^* &= \dfrac{\alpha_1\left(\epsilon_0 h_d + \alpha_2 e^*\kappa(1-q)\right) + \nu_2\rho_0 h_d}{\nu_1\nu_2 h_d}. \end{cases} \tag{14}$$

Substituting the expressions (14) into the second equation of system (2) leads to the following third order polynomial equation in terms of e^*

$$e^*\left(ae^{*^2} + be^* + c\right) = 0 \tag{15}$$

where

$$\begin{cases} a &= \alpha_1\alpha_2\beta\kappa^2(1-q)(\kappa+\mu)\left(\eta q h_d + (1-q)h_u\right), \\ b &= -\beta\kappa\left(\eta q h_d + (1-q)h_u\right)\left(h_d\nu_1\nu_2(\mu+\kappa)(1-\Phi) + \mu\kappa\alpha_1\alpha_2(1-q)\right), \\ c &= \mu h_d^2 h_u\nu_1\nu_2(\mu+\kappa)\left[\mathcal{R}_0 - 1\right]. \end{cases} \tag{16}$$

Solving (15) gives $e^* = 0$ which corresponds to the disease-free equilibrium or

$$ae^{*^2} + be^* + c = 0. \tag{17}$$

We solve the quadratic equation (17). Note that

$$a > 0, \qquad b < 0, \qquad c > 0 \ \ (\mathcal{R}_0 > 1) \quad \text{and} \quad c < 0 \ \ (\mathcal{R}_0 < 1). \tag{18}$$

Various possibilities for the existence of the endemic equilibrium are shown in the Table below. Here, i^* denotes the number of roots of (17). Thus, we summarise results on the existence of the endemic equilibrium of system (2)-(3) in Theorem 1.

Preprints (www.preprints.org) | NOT PEER-REVIEWED | Posted: 7 November 2022 doi:10.20944/preprints202211.0100.v1

	$a>0$	
	$b<0$	
	$c>0$ $(R_0>1)$	$c<0$ $(R_0<1)$
i^*	2	1

Theorem 1. $(\mathcal{H}_1)$. *System* (2)-(3) *has a unique endemic equilibrium* $\mathcal{D}^* = (s^*, e^*, i_u^*, i_d^*, r_u^*, r_d^*, \rho^*, \epsilon^*)$ *if and only if* $a > 0$, $b < 0$ *and* $\mathcal{R}_0 < 1$.

$(\mathcal{H}_2)$. *System* (2)-(3) *has two endemic equilibria* $\mathcal{D}_1^* = (s_1^*, e_1^*, i_{u1}^*, i_{d1}^*, r_{u1}^*, r_{d1}^*, \rho_1^*, \epsilon_1^*)$ *and* $\mathcal{D}_2^* = (s_2^*, e_2^*, i_{u2}^*, i_{d2}^*, r_{u2}^*, r_{d2}^*, \rho_2^*, \epsilon_2^*)$ *if and only if* $a > 0$, $b < 0$ *and* $\mathcal{R}_0 > 1$.

3.5 Local stability of the endemic equilibrium point

In this section, we study the local stability of the endemic equilibrium of system (2)-(3). We employ Theorem 4.1 proven in the work by Castillo-Chavez and Song [5]. We focus on the application of the theorem and refer readers to [5] for more details on the theorem. We introduce the following change of variables for easy application of Theorem 4.1:
$s = x_1$, $e = x_2$, $i_d = x_3$, $i_u = x_4$, $r_d = x_5$, $r_u = x_6$, $\rho = x_7$, $\epsilon = x_8$, so that $\mathrm{N} = \sum_{n=1}^{8} x_n$. We now use the vector notation $X = (x_1, x_2, x_3, x_4, x_5, x_6, x_7, x_8)^T$. Then, model system (2)-(3) can be written in the form

$$\frac{dX}{dt} = F(t, x(t)) = (f_1, f_2, f_3, f_4, f_5, f_6, f_7, f_8)^T,$$

where

$$\left.\begin{aligned}
\frac{dx_1}{dt} &= \mu - \beta(1-\rho)(x_3 + \eta x_4)x_1 - \mu x_1 = f_1,\\
\frac{dx_2}{dt} &= \beta(1-\rho)(x_3 + \eta x_4)x_1 - (\mu+\kappa)x_2 = f_2,\\
\frac{dx_3}{dt} &= (1-q)\kappa x_2 - h_d x_3 = f_3,\\
\frac{dx_4}{dt} &= q\kappa x_2 - h_u x_4 = f_4,\\
\frac{dx_5}{dt} &= \sigma_d x_3 - \mu x_5 = f_5,\\
\frac{dx_6}{dt} &= \sigma_u x_4 - \mu x_6 = f_6,\\
\frac{dx_7}{dt} &= \rho_0 + \alpha_1 x_8 - \nu_1 x_7 = f_7,\\
\frac{dx_8}{dt} &= \epsilon_0 + \alpha_2 x_3 - \nu_2 x_8 = f_8.
\end{aligned}\right\} \quad (19)$$

Preprints (www.preprints.org) | NOT PEER-REVIEWED | Posted: 7 November 2022 doi:10.20944/preprints202211.0100.v1

Let β be the bifurcation parameter, $\mathcal{R}_0 = 1$ corresponds to

$$\beta = \beta^* = \frac{\nu_1\nu_2 h_d h_u(\kappa+\mu)}{\kappa\left(\nu_2\left(\nu_1-\rho_0\right)-\alpha_1\epsilon_0\right)\left(\eta q h_d+(1-q)h_u\right)}. \tag{20}$$

The Jacobian matrix of system (2)-(3) at $\mathcal{D}^0$ when $\beta = \beta^*$ is given by

$$J^*(\mathcal{D}^0) = \begin{pmatrix} -\mu & 0 & -\beta^*(1-\Phi) & -\beta^*\eta(1-\Phi) & 0 & 0 & 0 & 0 \\ 0 & -\kappa-\mu & \beta^*(1-\Phi) & \beta^*\eta(1-\Phi) & 0 & 0 & 0 & 0 \\ 0 & (1-q)\kappa & -h_d & 0 & 0 & 0 & 0 & 0 \\ 0 & q\kappa & 0 & -h_u & 0 & 0 & 0 & 0 \\ 0 & 0 & \sigma_d & 0 & -\mu & 0 & 0 & 0 \\ 0 & 0 & 0 & \sigma_u & 0 & -\mu & 0 & 0 \\ 0 & 0 & 0 & 0 & 0 & 0 & -\nu_1 & \alpha_1 \\ 0 & 0 & \alpha_2\epsilon_0 & 0 & 0 & 0 & 0 & -\nu_2 \end{pmatrix}$$

where h_d and h_u are defined as before.
It can be noted that for $\beta = \beta^*$, system (2)-(3) has a simple eigenvalue. Thus, the center manifold theory can be applied to analyse the dynamics of system (2)-(3) near $\beta = \beta^*$. The right eigenvector for $J^*(\mathcal{D}^0)$ is given by $w = (w_1, w_2, w_3, w_4, w_5, w_6, w_7, w_8)^T$, where

$$\begin{aligned} w_1 &= \nu_1\nu_2 h_d h_u(\kappa+\mu), \quad w_2 = -\mu\nu_1\nu_2 h_d h_u, \quad w_3 = -\kappa\mu\nu_1\nu_2(1-q)h_u, \\ w_4 &= -\kappa\mu\nu_1\nu_2 q h_d, \quad w_5 = -\kappa\nu_1\nu_2(1-q)\sigma_d h_u, \quad w_6 = -\kappa\nu_1\nu_2 q h_d\sigma_u, \\ w_7 &= -\alpha_1\alpha_2\kappa\mu(1-q)\epsilon_0 h_u, \quad w_8 = -\alpha_2\kappa\mu\nu_1(1-q)\epsilon_0 h_u. \end{aligned}$$

The left eigenvector of $J^*(\mathcal{D}^0)$, associated with the zero eigenvalue at $\beta = \beta^*$ is given by $v = (v_1, v_2, v_3, v_4, v_5, v_6, v_7, v_8)^T$, where

$$\begin{aligned} v_1 &= v_5 = v_6 = v_7 = v_8 = 0, \quad v_2 = \kappa\left(\eta q h_d + (1-q)h_u\right), \\ v_3 &= h_u(\kappa+\mu), \quad v_4 = \eta h_d(\kappa+\mu). \end{aligned}$$

Now, we compute **a** and **b** and apply Theorem 4.1 in Castillo-Chavez and Song [5]. For system (19), the associated non-zero partial derivatives of F at $\mathcal{D}^0$ are given

Preprints (www.preprints.org) | NOT PEER-REVIEWED | Posted: 7 November 2022 doi:10.20944/preprints202211.0100.v1

below in (21).

$$\begin{cases} \dfrac{\partial^2 f_1}{\partial x_1 \partial x_3} = \dfrac{\partial^2 f_1}{\partial x_3 \partial x_1} = -\beta^* (1-\Phi), \quad \dfrac{\partial^2 f_1}{\partial x_1 \partial x_4} = \dfrac{\partial^2 f_1}{\partial x_4 \partial x_1} = -\beta^* \eta (1-\Phi), \\ \dfrac{\partial^2 f_1}{\partial x_3 \partial x_7} = \dfrac{\partial^2 f_1}{\partial x_7 \partial x_3} = \beta^*, \quad \dfrac{\partial^2 f_1}{\partial x_4 \partial x_7} = \dfrac{\partial^2 f_1}{\partial x_7 \partial x_4} = \eta \beta^*, \\ \dfrac{\partial^2 f_2}{\partial x_1 \partial x_3} = \dfrac{\partial^2 f_2}{\partial x_3 \partial x_1} = \beta^* (1-\Phi), \quad \dfrac{\partial^2 f_2}{\partial x_1 \partial x_4} = \dfrac{\partial^2 f_2}{\partial x_4 \partial x_1} = \beta^* \eta (1-\Phi), \\ \dfrac{\partial^2 f_2}{\partial x_3 \partial x_7} = \dfrac{\partial^2 f_2}{\partial x_7 \partial x_3} = -\beta^*, \quad \dfrac{\partial^2 f_2}{\partial x_4 \partial x_7} = \dfrac{\partial^2 f_2}{\partial x_7 \partial x_4} = -\eta \beta^*, \\ \dfrac{\partial^2 f_1}{\partial x_3 \partial \beta^*} = \Phi - 1, \quad \dfrac{\partial^2 f_1}{\partial x_4 \partial \beta^*} = -\eta (1-\Phi), \\ \dfrac{\partial^2 f_2}{\partial x_3 \partial \beta^*} = 1 - \Phi, \quad \dfrac{\partial^2 f_2}{\partial x_4 \partial \beta^*} = \eta (1-\Phi). \end{cases} \tag{21}$$

It thus follows that

$$\begin{aligned} \mathbf{a} &= \sum_{i=3}^{4} 2 v_2 w_1 w_i \frac{\partial^2 f_2}{\partial x_1 \partial x_i} + \sum_{i=3}^{4} 2 v_2 w_7 w_i \frac{\partial^2 f_2}{\partial x_i \partial x_7} \\ &= \xi_1 (\xi_2 - \xi_3) \\ &= \xi_1 \xi_3 (\Delta - 1) \quad \left(\frac{\xi_2}{\xi_3} = \Delta \right), \end{aligned}$$

where

$$\begin{aligned} \xi_1 &= 2\beta\kappa\mu\nu_1\nu_2 h_u (\eta q h_d + (1-q) h_u), \\ \xi_2 &= h_d^2 \nu_1 \nu_2 (\kappa + \mu)(\Phi - 1)(h_u + \eta\kappa q), \\ \xi_3 &= \alpha_1\alpha_2\eta\kappa^2\mu(1-q)q\epsilon_0 h_d + \alpha_1\alpha_2\kappa^2\mu(1-q)^2\epsilon_0 h_u. \end{aligned}$$

Now, we fix $\rho_0 > \nu_1$. Note that if $\Delta > 1$, then $\mathbf{a} > 0$ and $\mathbf{a} < 0$ if $\Delta < 1$. Lastly,

$$\mathbf{b} = \kappa^2 \mu (\alpha_1 \epsilon_0 + \nu_2 (\rho_0 - \nu_1)) (\eta q h_d + (1-q) h_u)^2 > 0.$$

We thus have the following result

Theorem 2. *If $\Delta < 1$ the endemic equilibrium of system (2)-(3) is locally asymptotically stable for $\mathcal{R}_0 > 1$ but close to one. Otherwise, if $\Delta > 1$, then model system (2)-(3) has a backward bifurcation at $\mathcal{R}_0 = 1$.*

4 Numerical simulations and model validation

The population of South Africa in 2020 was estimated to be 59.54 million [17]. We take the initial time of the epidemic to be the time when the first lock down

Preprints (www.preprints.org) | NOT PEER-REVIEWED | Posted: 7 November 2022 doi:10.20944/preprints202211.0100.v1

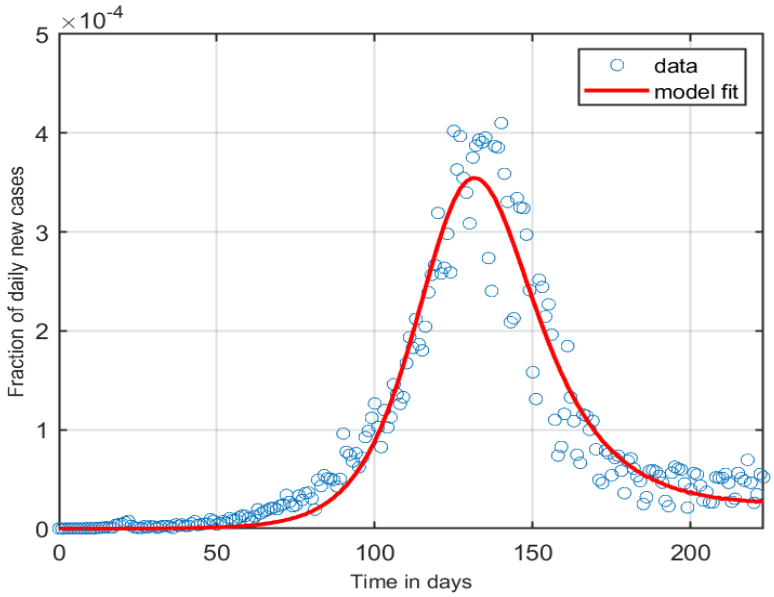

Figure 2: A figure showing the model fitted to the first wave of the epidemic in South Africa for the following parameter values: $\mu = 0.01,\ \beta = 2.6060,$ $\eta = 0.4651,\ \ q = 0.9571,\ \kappa = 0.3143,\ \sigma_u = 0.54511,\ \sigma_d = 0.9649,\ \alpha_1 = 0.0050,$ $\alpha_2 = 0.0842,\ \delta_u = 0.1693,\ \delta_d = 0.5033,\ \nu_1 = 0.0957,\ \nu_2 = 0.0100,\ \rho_0 = 0.0122.$

measures took effect, i.e on the 27^{th} of March 2020. The choice of the initial time is driven by the fact that there were no non-pharmaceutical interventions before then. Also, the waves following the first wave had additional interventions that included vaccination, which were not captured in our model. It is thus apparent that we use data from the first wave. We chose the end time of the first wave to be the 15^{th} of October 2020. It is important that there was no clear time set for the end of the first wave and the start of the second wave. We hypothetically chose a value at the mid-point of trough between the first and second waves. The initial conditions are given by

$$\begin{aligned} s0 =& \frac{59539894}{59540000},\ e_0 = \frac{86}{59540000},\ I_{d0} = \frac{20}{59540000},\ I_{u0} = 0, \\ r_{d0} =& 0,\ r_{u0} = 0,\ \rho_0 = 0,\ \epsilon_0 = 0. \end{aligned}$$

While some of the parameters such as the birth/death rates can be obtained from [17], the majority of the parameters are generated by the curve fitting algorithm, the *fminsearch*, which uses the Nelder-Mead simplex algorithm described in detail in [14]. The birth/death rate in this case is assumed to be related to the life expectancy in the year 2020. The life expectancy in South Africa was 65.5 years in the year 2020, translating to $\mu = 0.015$. The number of undetected cases is estimated to be seven times higher than the reported figures [29]. So q is chosen in such away that the proportion of undetected cases is seven times that of the detected. We thus have $q = 0.875$. Our fitting suggest a value three times the one reported in [29] for South Africa. The remaining parameters are determined from the fitting.

Preprints (www.preprints.org) | NOT PEER-REVIEWED | Posted: 7 November 2022 doi:10.20944/preprints202211.0100.v1

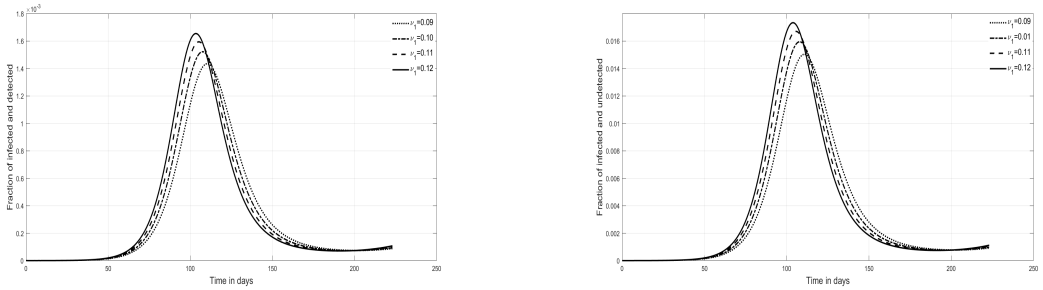

(a) (b)

Figure 3: (a) The fraction of detected cases (b) The fraction of undetected cases as ν_1 varies. The subfigures show that the number of cases increase with any increase in the reduction of NPIs.

4.1 Impact of varying NPIs

NPIs were impacted greatly when changes in the lockdown levels as the COVID-19 pandemic progressed continued. Relaxations and tightening of NPIs has been the norm in many countries depending on the number of cases and changes in hospitalisation levels over time. We consider the relaxation of interventions that are impacted by fear. As the numbers of cases decrease, the fear of COVID-19 decreases and consequently leading to a relaxation of the NPIs. The impact of NPIs is modelled by the parameter ν_1.

4.2 Impact of varying fear levels

The structure of our model is such that fear resulting from increased numbers of detected cases can give rise to increased NPIs. The removal in the levels for fear is modeled by the parameter ν_2. We vary ν_2 from 0.1 to 0.7 and the fraction of undetected infectives follows the dynamics in Figure 4. Clearly, the direct impact of fear does not translate into significant changes in the fraction of infectives. We had to zoom in to determine the influence of varying ν_2. The insert on Figure 4 shows that increasing the levels of fear results in increased number of infected cases.

4.3 Impact of varying parameters ν_1 and κ on R_0.

The reduction in the NPIs, modelled by ν_1 and the progression to infectiousness, modelled by κ is of interest. We determine the effects of both parameters by a contour plot R_0 and the two parameters. Figure 5 shows that an increase in the two parameters leads to an increase in the value of R_0. We add a surface of $R_0 = 1$, to establish the parameter values of ν_1 and κ for which the value of $R_0 = 1$. This is key in determining the persistence of the infection when all other parameters are assumed to be constant.

Preprints (www.preprints.org) | NOT PEER-REVIEWED | Posted: 7 November 2022 doi:10.20944/preprints202211.0100.v1

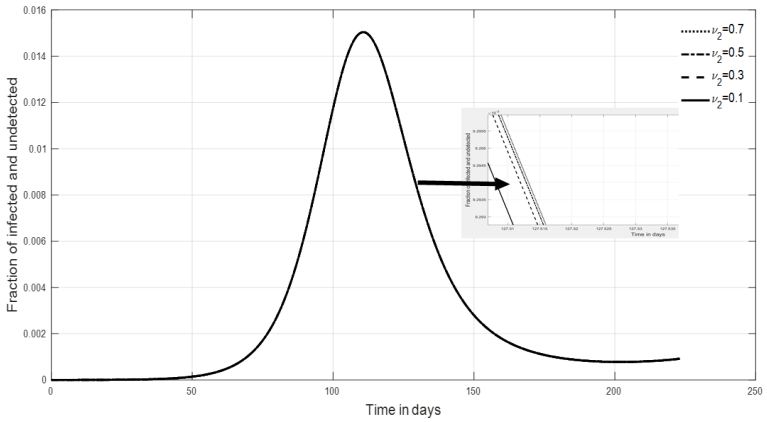

Figure 4: A figure showing the effects of varying ν_2.

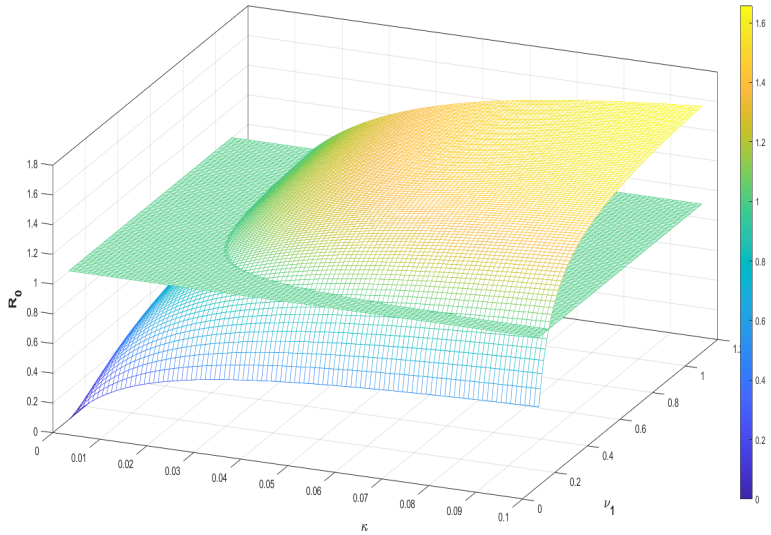

Figure 5: shows a contour plot for the parameters κ and η.

4.4 Impact varying parameters α_1 and β on R_0.

Preprints (www.preprints.org) | NOT PEER-REVIEWED | Posted: 7 November 2022 doi:10.20944/preprints202211.0100.v1

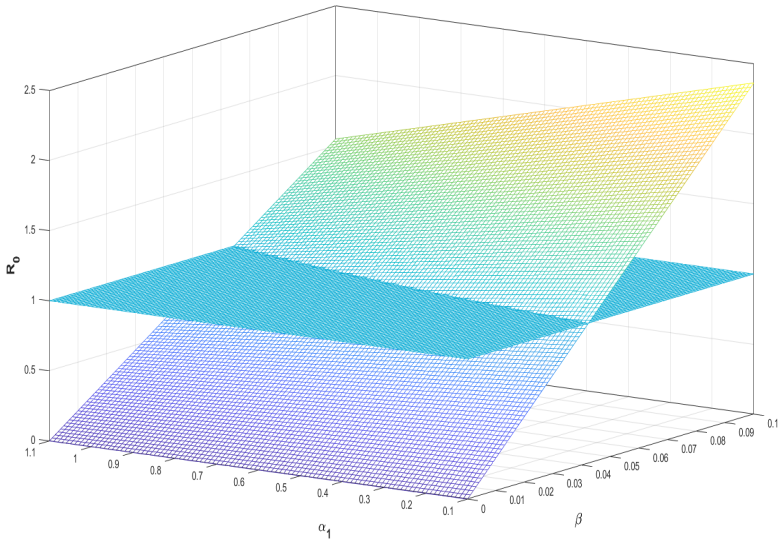

Figure 6: shows a contour plot for the parameters α_1 and β.

5 Conclusion

The work considered in this study captures the role of human behavior on the spread of COVID-19 in South Africa influenced by spread of information. An eight-state system of ODEs split into two sub-systems capturing human dynamics and social dynamics is formulated. As can be observed in the social dynamics sub-system, information on COVID-19 is considered to depend on data for COVID-19 detected cases which in turn influence changes in human behavior. Baseline values for information availability and human behavior are included to add realism to the system of equations. Theoretical and numerical analysis of the model is carried out. The model is applied to data on COVID-19 dynamics in South Africa with first wave data used to validate the model.

Mathematical models that include human behaviour are key to the management of diseases. COVID-19 treatment remain part of a bigger global research drive to find therapeutics for the disease. In the mean time, the management and control of the disease relied on human behaviour influenced by government policies. In South Africa, restrictions to human movement, personal hygiene, cleaning of surfaces, sanitizing and social distancing were key to minimising transmission before the advent of the vaccines on the market. In particular, regulations on restrictions varied as lockdown levels changed depending on the number of cases and hospitalization rates.

Other functions for $f(\epsilon)$ and $g(\frac{I_d}{N})$ can be used to model the growth of NPIs and fear other than the ones presented in this article. One of the weaknesses of this article is the non inclusion of the hospitalised compartment, who can influence the information that impacts the dynamics of the NPIs. The paper can also be extended to incorporate vaccination as many countries to date have considered this as the main preventive form of control for COVID-19. These aspects and some other observed characteristics that influence the trends of spread of COVID-19 can be considered

as possible extensions to this work.

Acknowledgements

The authors are very grateful to the anonymous reviewers for their careful reading and constructive comments. The authors are also grateful for the support rendered by their respective institutions towards the production of the manuscript.

Funding

The authors received no funding for this research work.

Conflicts of Interest

The authors declare that there is no conflict of interest regarding the publication of this article plain

References

[1] Fulk Alexander Abu-Saymeh Daniel Romero-Alvarez Qays Ponce Joan Sindi Suzanne Ortega Omayra Saint Onge Jarron M. Agusto Folashade B. Erovenko Igor V. and Peterson A. Townsend, *To isolate or not to isolate: the impact of changing behavior on covid-19 transmission*, BMC Public Health **22** (2022), 138.

[2] M. Ashour, K. Bekiroglu, C. Yang, C. Lagoa, D. Conroy, J. Smyth, and S. Lanza, *On the mathematical modeling of the effect of treatment on human physical activity*, 2016 ieee conference on control applications (cca), 2016Sep., pp. 1084–1091.

[3] Rachel E. Baker, Sang Woo Park, Wenchang Yang, Gabriel A. Vecchi, C. Jessica E. Metcalf, and Bryan T. Grenfell, *The impact of covid-19 nonpharmaceutical interventions on the future dynamics of endemic infections*, Proceedings of the National Academy of Sciences **117** (2020), no. 48, 30547–30553, available at `https://www.pnas.org/content/117/48/30547.full.pdf`.

[4] Andrea L. Bertozzi, Elisa Franco, George Mohler, Martin B. Short, and Daniel Sledge, *The challenges of modeling and forecasting the spread of covid-19*, Proceedings of the National Academy of Sciences **117** (2020), no. 29, 16732–16738, available at `https://www.pnas.org/content/117/29/16732.full.pdf`.

[5] Carlos Castillo-Chavez and Baojun Song, *Dynamical models of tuberculosis and their applications*, Mathematical Biosciences & Engineering **1** (2004), no. 2, 361.

[6] Ian Cooper, Argha Mondal, and Chris G. Antonopoulos, *A sir model assumption for the spread of covid-19 in different communities*, Chaos, solitons, and fractals **139** (2020), 110057–110057, available at `https://doi.org/10.1080/22221751.2020.1760146`.

[7] Johnston Matthew D. and Pell Bruce, *A dynamical framework for modeling fear of infection and frustration with social distancing in covid-19 spread*, Mathematical Biosciences and Engineering **17** (2020), no. 6, 7892–7915.

[8] Camila Alves dos Santos Siqueira, Yan Nogueira Leite de Freitas, Marianna de Camargo Cancela, Monica Carvalho, Albert Oliveras-Fabregas, and Dyego Leandro Bezerra de Souza, *The effect of lockdown on the outcomes of covid-19 in spain: An ecological study* **15** (2020), no. 7, e0236779.

[9] KJ Friston, T Parr, P Zeidman, A Razi, G Flandin, J Daunizeau, OJ Hulme, AJ Billig, V Litvak, CJ Price, RJ Moran, and C Lambert, *Second waves, social distancing, and the spread of covid-19 across america [version 1; peer review: 2 approved with reservations]*, Wellcome Open Research **5** (2020), no. 103.

[10] Sebastiann Funk, Marcel Salathe, and Vincent A A Jansen, *Modelling the influence of human behaviour on the spread of infectious diseases: a review*, Journal of the Royal Society, Interface **7** (2020), no. 50, 1247 –1256.

[11] Giulia Giordano, Franco Blanchini, Patrizio Colaneri Raffaele Bruno, Alessandro Di Filippo, Angela Di Matteo, and Marta Colaneri, *Modelling the covid-19 epidemic and implementation of population-wide interventions in italy*, Nature Medicine **26** (2020), 855 – 860.

[12] Lara Goscé, Andrew Phillips, P. Spinola, Rishi K. Gupta, and Ibrahim Abubakar, *Modelling sars-cov2 spread in london: Approaches to lift the lockdown* **82** (2020), no. 2, 260 – 265.

[13] Antonio Guirao, *The covid-19 outbreak in spain. a simple dynamics model, some lessons, and a theoretical framework for control response*, Infectious Disease Modelling **5** (2020), 652 –669.

[14] J. C. Lagarias, Reeds J. A., Wright M. H., and Wright P. E., *Convergence properties of the nelder-mead simplex method in low dimensions*, SIAM Journal of Optimization **9** (1998), no. 1, 112–147.

[15] M. Liu, J. Ning, Y. Du, J. Cao, D. Zhang, J. Wang, and M. Chen, *Modelling the evolution trajectory of covid-19 in wuhan, china: experience and suggestions*, Public Health **183** (2020), 76 –80.

[16] Magal P. Seydi O. Liu Z. and G. Webb, *A covid-19 epidemic model with latency period*, Infectious Disease Modelling **5**.

[17] R. Maluleke, *Mid-year population estimates 2021*, 2022. Accessed: 2022-02-04.

[18] Philip Nadler, Shuo Wang, Rossella Arcucci, Xian Yang, and Yike Guo, *An epidemiological modelling approach for covid-19 via data assimilation*, European Journal of Epidemiology **35** (2020), no. 8, 749 –761.

[19] Chukwu C.W. Visaya M.V. Nyabadza F. Chirove F., *Modelling the potential impact of social distancing on the covid-19 epidemic in south africa*, Computational and Mathematical Methods in Medicine **2020, Article ID 5379278** (2020), 12 pages.

[20] U.S. Department of Health & Human Services, *Covid-19 treatments and therapeutics, year = 2022, eprint = https://www.hhs.gov/coronavirus/covid-19-treatments-therapeutics/index.html, note = Accessed: 2022-04-08.*

[21] Sylvester Maleghemi-John Rumunu David Ameh Olushayo Oluseun Olu Joy Luba Lomole Waya and Joseph Francis Wamala, *Moving from rhetoric to action: how africa can use scientific evidence to halt the covid-19 pandemic*, Infectious Diseases of Poverty **9** (2020).

[22] Sansao A Pedro, Frank T Ndjomatchoua, Peter Jentsch, Jean M Tcheunche, Madhur Anand, and Chris T Bauch, *Conditions for a second wave of covid-19 due to interactions between disease dynamics and social processes.*

[23] Tim Rhodes, Kari Lancaster, Shelley Lees, and Melissa Parker, *Modelling the pandemic: attuning models to their contexts*, BMJ Global Health **5** (2020), no. 6, available at `https://gh.bmj.com/content/5/6/e002914.full.pdf`.

[24] Bossert A. Kersting M. et al Schröder M., *Covid-19 in south africa: outbreak despite interventions*, Scientific Reports **11** (2021), 956.

[25] Lone Simonsen, Gerardo Chowell, Viggo Andreasen, Robert Gaffey, John Barry, Don Olson, and Cécile Viboud, *A review of the 1918 herald pandemic wave: importance for contemporary pandemic response strategies*, Annals of Epidemiology **28** (2018), no. 5, 281 –288. Special Issue on Pandemic Influenza.

[26] Fallani S. Voller F. Stasi C. and C. Silvestri, *Treatment for covid-19: An overview*, European Journal of Pharmacology **889** (2020), 173644.

[27] Richard O. J. H. Stutt, Renata Retkute, Michael Bradley, Christopher A. Gilligan, and John Colvin, *A modelling framework to assess the likely effectiveness of facemasks in combination with ‘lock-down’ in managing the covid-19 pandemic*, Proceedings of the Royal Society A: Mathematical, Physical and Engineering Sciences **476** (2020), no. 2238, 20200376, available at `https://royalsocietypublishing.org/doi/pdf/10.1098/rspa.2020.0376`.

[28] Yuanji Tang and Shixia Wang, *Mathematic modeling of covid-19 in the united states*, Emerging Microbes & Infections **9** (2020), no. 1, 827–829, available at `https://doi.org/10.1080/22221751.2020.1760146`. PMID: 32338150.

[29] Burki T.K., *Undetected covid-19 cases in africa*, The Lancet Respiratory Medicine **9** (2021), no. 12, e121.

[30] Pauline Van den Driessche and James Watmough, *Reproduction numbers and sub-threshold endemic equilibria for compartmental models of disease transmission*, Mathematical biosciences **180** (2002), no. 1-2, 29–48.

[31] Caroline E. Walters, Margaux M.I. Meslé, and Ian M. Hall, *Modelling the global spread of diseases: A review of current practice and capability*, Epidemics **25** (2018), 1 –8.

[32] Worldometer., *Covid-19 coronavirus pandemic, year = 2022, eprint = https://www.worldometers.info/coronavirus/, note = Accessed: 2022-04-08.*

[33] Joseph T Wu, Kathy Leung, and Gabriel M Leung, *Nowcasting and forecasting the potential domestic and international spread of the 2019-ncov outbreak originating in wuhan, china: a modelling study*, The Lancet **395** (2020), no. 10225, 689 –697.